JACS
JOURNAL OF THE AMERICAN CHEMICAL SOCIETY

Article

pubs.acs.org/JACS

Self-Organization of Bent Rod Molecules into Hexagonally Ordered Vesicular Columns

Ho-Joong Kim,[†,‡] Feng Liu,[∥,‡] Ja-Hyoung Ryu,[†,‡] Seong-Kyun Kang,[†] Xiangbing Zeng,[∥] Goran Ungar,*[,§,∥] Jeong-Kyu Lee,[⊥] Wang-Cheol Zin,[⊥] and Myongsoo Lee*[,†]

[†]Center for Supramolecular Nano-Assembly and Department of Chemistry and [§]School of Chemical and Biological Engineering, WCU Program of Chemical Convergence for Energy and Environment, Seoul National University, Seoul 151-747, Korea

[∥]Department of Materials Science and Engineering, University of Sheffield, Mappin Street, Sheffield S1 3JD, United Kingdom

[⊥]Department of Materials Science and Engineering, Polymer Research Institute, Pohang University of Science and Technology, Pohang 790-784, Korea

S *Supporting Information*

ABSTRACT: Bent-shaped rigid-core molecules with flexible chiral dendrons grafted to the outer side of the bend were synthesized and characterized by circular dichroism, differential scanning calorimetry, X-ray scatterings, and transmission electron microscopy in solution and the solid state. The bent aromatic rods based on hepta- and nonaphenylene with nitrile groups at both ends self-assemble into well-ordered hollow tubular structures in aqueous solution, while the bent rod based on heptaphenylene without nitrile groups showed no apparent aggregations in aqueous solution. In the solid state, the rigid-flexible molecules based on heptaphenylene rod without the nitrile group self-assemble into a 2D oblique columnar structure with the columnar cross-section containing two interlocked molecules. Remarkably, the rigid flexible molecules based on hepta-, nona-, and undecaphenylene with nitrile groups self-assemble into a hexagonal columnar structure with weak 3D order. A model of vesicular channel structure is proposed based on small- and wide-angle X-ray diffraction on oriented fibers, density measurement, reconstruction and simulation of electron density maps, and molecular dynamics simulation. In contrast to the hollow tubular structure found in solution, in the solid both the outside and the interior of the columns are filled by the pendant aliphatic coils. Filling of the interior of these vesicular channels is made possible by some bent rod molecules turning their obtuse apex inward. One in 7, 2 in 8, and 4 in 10 molecules are thus inverted in a column slice in compounds with hepta-, nona-, and undecaphenylene cores, respectively. These are new examples of vesicular double-segregated columnar structures recently discovered in some dendrons.

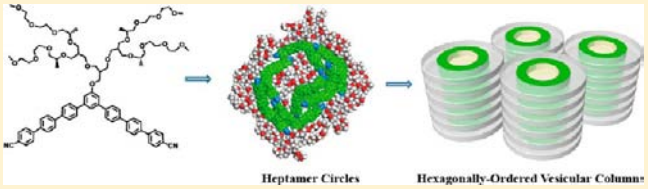

■ INTRODUCTION

Supramolecular assembly of elaborately designed molecules offers a new strategy for creating novel nanostructures with desired shape and size, which are important modules in the development of nanoclusters and biomaterials.[1] The diblock or triblock molecules, including block copolymers, amphiphilic rods, dendrons, and peptide derivatives, self-assemble into diverse nanostructures which are manipulated by precise control of molecular structure such as the type and relative length of the respective block.[2] Among the various supramolecular nanostructures, construction of channel-like structures has received enormous attention due to their application potentials in electro-optic materials, biological channel, and nanopatterning process.[3] For instance, the unique channel-like honeycombs have been developed in liquid crystal (LC) states by Tschierske and co-workers.[4] They have shown formation of a series of honeycomb-like channel structures from triangles via squares and pentagons to hexagons and giant cylinder structures through the self-assembly process from polyphilic molecules composed of a rigid aromatic core, polar end groups, and one or two hydrophobic lateral chains. In these LC arrays, the honeycomb frames are constructed by walls of parallel arranged aromatic rods aligned perpendicular to the resulting channels. Percec et al. pioneered construction of supramolecular porous columns with a hollow center ranging from a few Angstroms to a few nanometers using self-assembly of conical dendrons.[5] Furthermore, precise control of the apex length of the conical dendrons generates the doubly segregated supramolecular channel-like columns and vesicles exhibiting polyhedral shapes.[5e] Helicenes with pendant alkyl chains were shown to form 6-strand helical tubular liquid crystal columns with a nearly 1 nm central void.[5b]

Rod−coil block molecules consisting of rigid aromatic rod and flexible coil segments are excellent candidates for creating well-defined supramolecular structures via a process of spontaneous organization.[6] In contrast to coil−coil block molecules, aromatic rod−coil molecules can form well-ordered structures in spite of the low molecular weights because the anisometric molecular shape and stiff rod-like conformation of

Received: June 22, 2012
Published: July 24, 2012

   dx.doi.org/10.1021/ja3060904 | *J. Am. Chem. Soc.* 2012, 134, 13871−13880

Scheme 1. Synthesis of the Bent-Shaped Molecules[a]

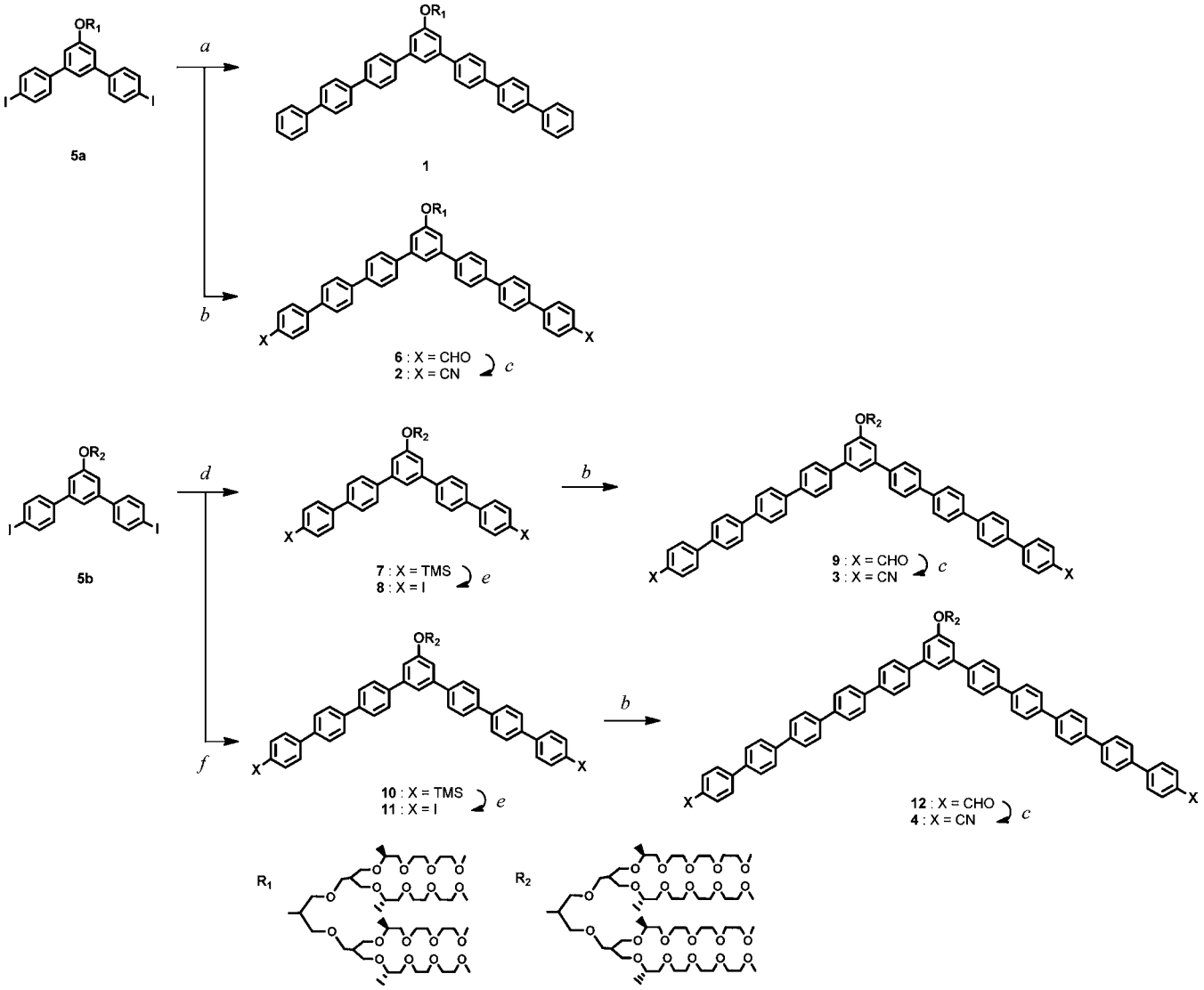

[a]Reagents and conditions: (a) biphenyl-4-ylboronic acid, $Pd(0)Ph_3P$, Na_2CO_3, H_2O, THF, reflux, 24 h; (b) 4′-formylbiphenyl-4-ylboronic acid, $Pd(0)Ph_3P$, Na_2CO_3, H_2O, THF, reflux, 24 h; (c) I_2, NH_3–H_2O, THF, rt, 1 h; (d) 4-trimethylsilyl-phenyl-boronic acid, $Pd(0)Ph_3P$, Na_2CO_3, H_2O, THF, reflux, 24 h; (e) 1.0 M ICl, CH_2Cl_2, −78 °C, 1 h; (d) 4-trimethylsilyl-biphenyl-boronic acid, $Pd(0)Ph_3P$, Na_2CO_3, H_2O, THF, reflux, 24 h.

the rod segment impart orientational organization. It has been also experimentally proven that systematic variation of the coil/rod volume fraction manipulates a variety of supramolecular nanostructures from lamellar, bicontinuous cubic, columnar, to cubic morphologies.[7] Recently, the rigid–flexible combination in a self-assembly system has been extended to laterally grafted bent rod molecules which self-assemble into a unique supramolecular structure, since assembly of bent rods would, in effect, give rise to a curved assembly as opposed to flat local structures.[8−10] For example, we have shown construction of 2D and 3D channel-like structures in bulk state from theself-assembly of laterally grafted bent-shaped molecules with an oligoether flexible chain at the internal bay position of the bent rods.[11] Six bent-shaped molecules self-assemble into hexameric macrocycles through a combination of shape complementarity and phase separation of dissimilar blocks, and then they stack into channel-like structures where the interiors are filled by the flexible oligoether chains. In addition, we recently communicated our preliminary findings on a hollow tubular structure that can be constructed by self-assembly of hexameric supramolecular macrocycles of the amphiphilic bent-shaped aromatic rod with an externally attached oligoether chain in aqueous solution.[12] The supramolecular macrocycles helically stack on top of one another to form water-soluble cylindrical tubules which self-dissociate into discrete toroidal stacks in response to salt addition. Since self-assembly of the laterally grafted bent rods can be used as a novel scaffold for shape-persistent macrocyclic frameworks in solution, we are interested in development of a unique channel-like structure in the solid state using bent rod molecules.

In this work, we investigate the solution and solid state structures of diblock molecules consisting of bent-shaped aromatic rods and oligoethyleneoxide dendritic segments, which forms a columnar structure with an amorphous channel from hierarchical assembly. Bent rods form a hexagonal columnar structure by assembling in a vesicle-like doubly segregated fashion. Fourier maps and model fitting of X-ray intensities reveal that while most aromatic cores bend inward

dx.doi.org/10.1021/ja3060904 | J. Am. Chem. Soc. 2012, 134, 13871−13880

with their dendrons facing out, some invert having their dendrons facing inward and filling the hollow interior of the tubular structure.

RESULTS AND DISCUSSION

Synthesis. Synthesis of the bent rod molecules was performed with preparation of a phenolic intermediate starting from a Suzuki coupling reaction with a 2,6-dibromophenol derivative and trimethylsilyl-substituted phenylboronic acids (Scheme 1). The bent-shaped scaffolds were synthesized by an etherification reaction of an appropriate oligoether dendritic chain and a phenolic intermediate and then a Suzuki coupling reaction with a biphenylboronic acid for **1**. Similar to the synthetic method of that for **1**, compound **2** was synthesized by Suzuki coupling reactions with 4′-formylbiphenyl-4-boronic acid and subsequent reduction by iodine and ammonia–water. Design of compounds **2**–**4** focuses on construction of the bent-shaped cores with different rod lengths, that is, aromatic segments based on heptaphenylene, nonaphenylene, and undecaphenylene units. Suzuki coupling reaction with TMS-protected phenyl boronic acid or biphenyl boronic acid was used to increase the length of the bent rods, following iodination reaction with ICl. The final bent-shaped compounds **3** and **4** were synthesized by Suzuki coupling reactions with 4′-formylbiphenyl-4-ylboronic acid and subsequent reduction by iodine and ammonia–water. The resulting compounds were characterized by ^{1}H NMR spectroscopy and MALDI-TOF mass spectrometry and shown to be in full agreement with the expected chemical structures.

Structural Investigation of Aqueous Solutions. The self-assembling behavior of the bent-shaped molecules in aqueous solution was investigated using circular dichroism (CD) and transmission electron microscopy (TEM). Previously we showed that compound **2** self-assembled into hexameric macrocycles in aqueous solution by complementary electrostatic interactions between electron-withdrawing nitrile groups and electron-donating phenoxy groups.[12] The resulting macrocycles, subsequently, stack on top of each other with mutual rotations in the same direction to give rise to helical tubules. For a more systematic study of the hollow tubular structure in aqueous solutions, we investigated the solution self-assembling behavior with different bent rod molecules. Remarkably, compound **1** which has no functional group at either end of the rod segment is not soluble in aqueous solution. Note that the difference between **1** and **2** is only the presence of the nitrile at the ends of the rod segment. This indicates that the complementary electrostatic interaction between the rod end and the bay position of rod segments plays a key role in forming the well-ordered supramolecular structures. Compounds **2** and **3** which have the nitrile groups at the ends show the hollow tubular structures in TEM (Figure 1a,b). The hollow interior is clearly visible, and the diameter is highly monodisperse. The diameter increases from 6.5 to 7.5 nm when rod length increases from hepta- to nonaphenylene, respectively. Compound **4**, which has an undecaphenylene rod building block, showed poor solubility due to the high lipophilic volume fraction. Considering that CD spectra of the aqueous solution of **2** and **3** show a significant Cotton effect in the spectral region of the aromatic units (Figure 1c), we can envision that these elongated objects in water are one-handed helical tubules. This indicates that the molecular chirality is transferred to the supramolecular assembly.

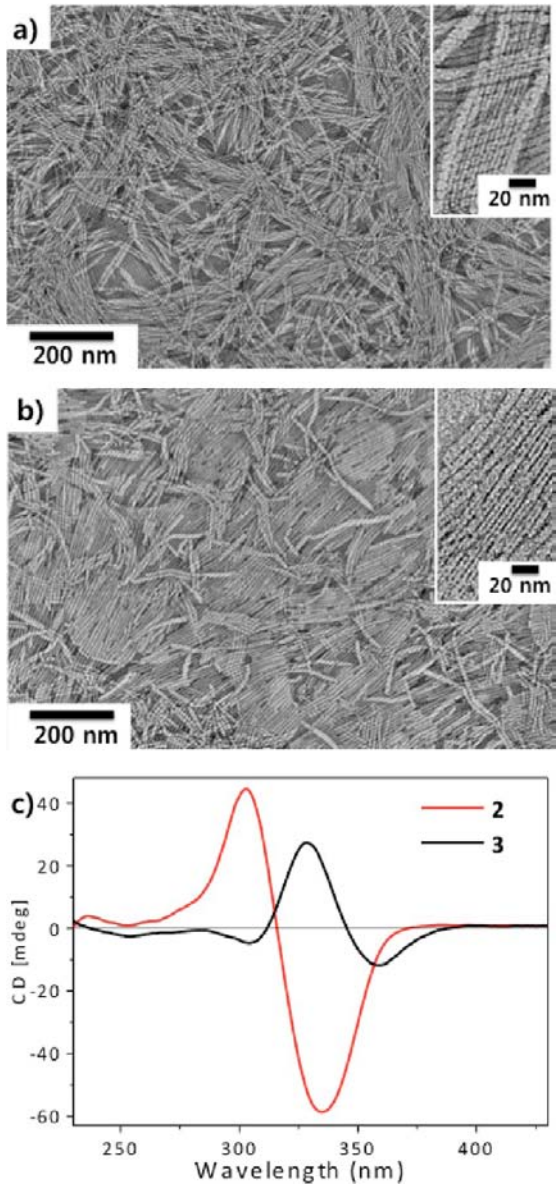

Figure 1. TEM images of **2** (a) and **3** (b) from 0.02 wt % aqueous solution (stained with uranyl acetate). (Insets) Tube with dark interior, indicative of hollow tubular objects. CD spectra of **2** (red line) and **3** (black line) (0.02 wt % aqueous solution) show a bisignated Cotton effect in the absorption region of the bent rods segments.

Highly concentrated aqueous solutions of compound **2** showed a birefringent texture which is typical of a liquid crystalline phase in a polarized optical microscope (POM). Since these aromatic macrocycles are surrounded by hydrophilic oligoether dendrons, they display a lyotropic phase in aqueous solution. Due to the presence of elongated stiff hexameric columns as shown in the TEM images (Figure 1a), **2** forms nematic liquid crystals in aqueous solution above 2 wt % (Figure 2a). As concentration increases above 60 wt %, the nematic fluid transforms into a hexagonal liquid crystal (Figure 2b). This lyotropic behavior in aqueous solution indicates that hexameric macrocycles are stable and form stiff rod-like cylinders.

Structural Investigation in the Solid State. The self-assembling behavior of the bent-shaped molecules in the bulk was investigated by means of differential scanning calorimetry

dx.doi.org/10.1021/ja3060904 | J. Am. Chem. Soc. 2012, 134, 13871–13880

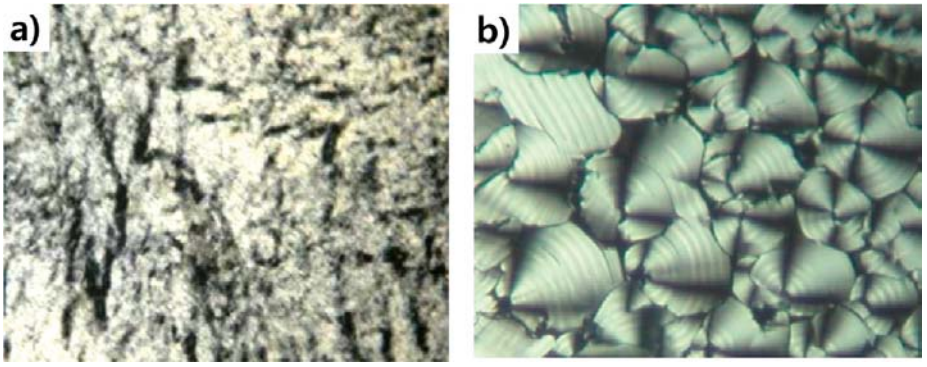

Figure 2. Optical polarized micrographs of the texture exhibited by (a) nematic phase of **2** in 2 wt % aqueous solution and (b) hexagonal columnar phase of **2** in 60 wt % aqueous solution.

(DSC), X-ray diffractions (XRD), and transmission electron microscopy (TEM). All of the compounds show an ordered structure, and the transition temperatures were determined from DSC scans (Figure 3). As the length of the bent rod

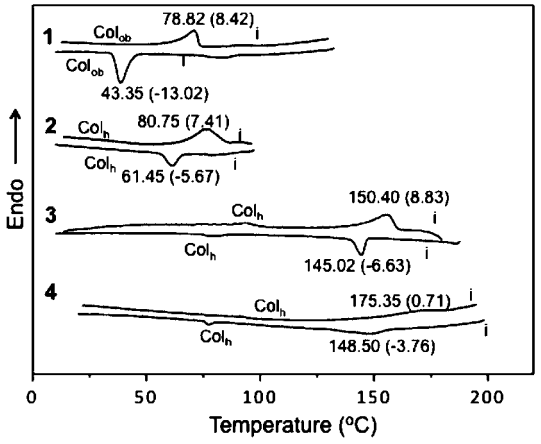

Figure 3. Second heating and first cooling differential scanning calorimetry traces of bent-shaped compounds **1**–**4** (10 °C/min). All samples were prepared from 3 mg of compounds in aluminum cells. Indium was used as a calibration standard. Phases, transition temperature (°C), and associated enthalpy change (kcal/mol) are indicated. Col$_{ob}$ = oblique columnar phase; Col$_h$ = hexagonal phase; i = isotropic.

increases, the melting (isotropization) point increases, indicating that the ordered structure becomes more stable, presumably due to increasing interaction between rod segments, including hydrophobic and $\pi-\pi$ interactions.

As confirmed by small-angle X-ray scatterings (SAXS), **1** based on a heptaphenylene aromatic segment self-assembles into an oblique columnar structure with lattice parameters a = 3.90 nm, b = 2.76 nm, and γ = 128.1° (Figure 4a and Table S1, Supporting Information). The wide-angle X-ray scattering (WAXS) pattern shows a weak but sharp reflection, indicating that the bent-shaped building blocks within the columns are $\pi-\pi$ stacked at a 0.46 nm distance along the column axis (Figure 4a, inset image). On the basis of the XRD results and measured density, the calculated number of molecules in a single slice of the column is about two (Table S7, Supporting Information). Therefore, we consider that the two bent rods in a single slice are packed in a dimeric associate in which the flexible chains surround the aromatic segments. This is supported by the reconstructed electron density map as

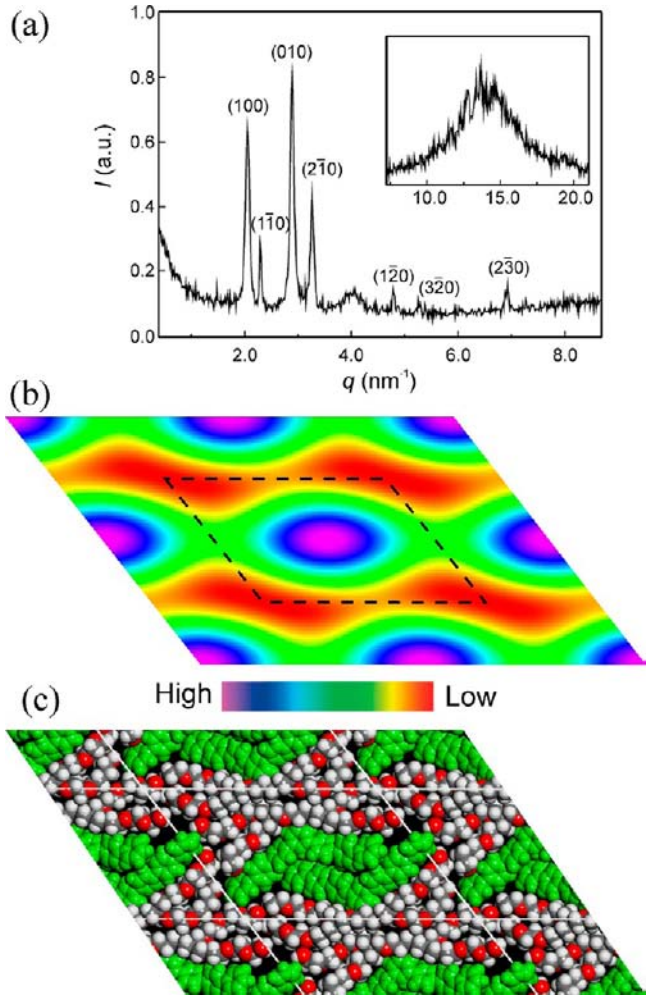

Figure 4. Compound **1**: (a) powder SAXS diffractogram (inset, WAXS). (b) Reconstructed electron density map of the oblique columnar phase (color scale at the bottom). (c) Snapshot after molecular dynamics annealing; aromatic cores are shown in green.

shown in Figure 4b (for the procedure see the Supporting Information). The map shows an elliptical column of high electron density (blue/purple) formed by the aromatic segments. Rows of these aromatic ribbons are separated by a layer of low electron density (yellow/red) which contains the aliphatic dendrons. To test the viability and space filling of this model further, molecular dynamics annealing was carried out. Two molecules of compound **1** were arranged in an oblique

dx.doi.org/10.1021/ja3060904 | J. Am. Chem. Soc. 2012, 134, 13871–13880

prism box with experimental lattice parameters and a height of 0.46 nm, under the 3-D periodic boundary condition. Thirty temperature cycles of constant volume (NVT) dynamics were run between 300 and 700 K, with a total annealing time of 30 ps, using the Forcyte module of Material Studio (Accelrys Inc.). Figure 4c shows a snapshot of one molecular layer (c = 0.46 nm) after annealing; the simulation is in fair agreement with the electron density map, confirming the efficient space filling and phase separation achieved by this structure.

Compounds **2**–**4** were functionalized at both ends of the aromatic core with nitrile groups. Addition of nitrile groups in compound **2**, which has otherwise the same heptaphenylene aromatic core as **1**, significantly changes the mode of molecular self-assembly. The SAXS pattern of **3** exhibits a number of sharp reflections corresponding to a 2D hexagonal lattice with a parameter a = 7.43 nm (Figure 5a and Table S3, Supporting Information). The SAXS patterns of **2**, based on a heptaphenylene aromatic segment, and **4**, based on an undecaphenylene aromatic segment, give similar SAXS patterns with a = 6.34 and 8.27 nm, respectively, see Figure S1 and Tables S2 and S4, Supporting Information.

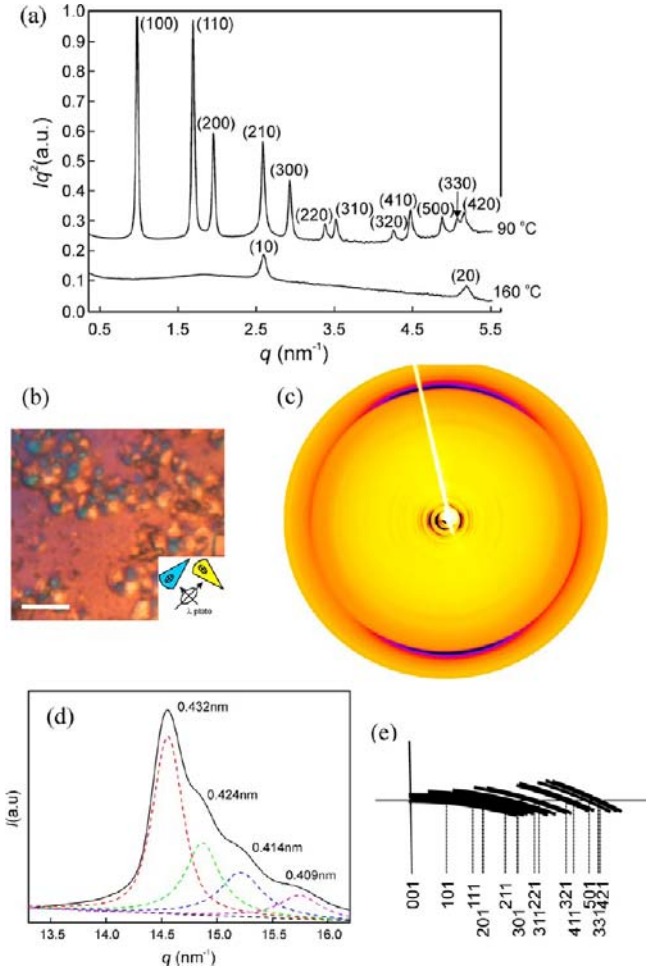

Figure 5. Compound **3**: (a) SAXS diffractiongrams recorded at 90 and 160 °C. Scattering curves are offset vertically for clarity. (b) Optical micrograph in the hexagonal phase between crossed polarizers and with a λ-plate retarder; indicatrix of the retarder is shown at bottom right; scale bar is 20 μm. (c) WAXS of a partially aligned sample at 90 °C (fiber axis vertical). (d) Radial scan of the fiber pattern in the limited wide-angle region of the π-stacking diffraction peaks ("first layer line"). (e) Drawn outline of the first layer line reflections (first quadrant) for a hypothetical fiber with a higher degree of orientation; figure shows clustering into four groups of unresolved reflections, observed as four components in d. This fixes the molecular spacing along the columns precisely at 0.43 nm (see Table S6, Supporting Information).

Figure 5b shows an optical micrograph of **3** in the hexagonal phase taken with crossed polarizers and a full-wave plate retarder. The orientation of the π-conjugated aromatic cores is deduced from the color of the fans in the "spherulites". The directions of yellow and blue fans with respect to the indicatrix of the retarder plate confirms the orientation of the high-index axis as radial to the fans. Since the columns are tangential and the high index axis is parallel to the oligophenylene long axis, it follows that the rod-like molecular cores are in the plane perpendicular to the column axis, which supports the column structure of these self-assemblies as described.

On the basis of our previous findings of hollow tubular structure in aqueous solution, we hypothesized similar packing in the solid state, i.e., that six bent-shaped aromatic segments might be arranged in a single slice with the terminal nitrile groups juxtaposed with the bay position of the adjacent molecule to form a hexameric macrocycle. The resulting macrocycles could stack on top of each other to form a hexagonal column structure with a hollow center, as depicted in Figure 6.

Another interesting feature of the SAXS patterns of **2**–**4** is the unusually strong high-order diffraction peaks of the hexagonal lattice. As previously reported, the enhanced diffraction peaks can be caused by the presence of a hollow or an electron-deficient center, reflected in the particular shape of the form factor of such columns. For example, the inverse hexagonal lyotropic liquid crystalline phases where the water channel in the core of the columns cause enhanced higher order peaks.[13] The cubic and columnar structures with hollow or aliphatic low electron density centers also show strong higher order reflections.[5] These qualitative considerations would seem to lend credence to the hexameric macrocycle model with a hollow center (Figure 6). However, such a packing model leaves a large empty space which is likely to be energetically prohibitive in solvent-free condensed matter. Of course, in addition to the form factor, another possible reason for intense higher diffraction orders is a high positional order parameter (Debye–Waller factor). The order is indeed likely to be higher than in classic "disordered" columnar liquid crystals since, as shown below, this hexagonal phase possesses a degree of 3-D long-range order.

Structural Investigation in Oriented Fiber. To investigate molecular assembly in the solid in more detail, we performed the following further studies. We measured the macroscopic density of the compounds, carried out X-ray scattering experiments on oriented fibers in the hexagonal columnar phase, reconstructed 2-D electron density maps from SAXS Bragg intensities, as well as simulated the diffraction patterns using geometric models and comparing the best-fit models with molecular models obtained by molecular dynamics (MD) simulation. This concerted effort was directed at answering the question of how the molecules were arranged in the column and particularly whether the inside of the column was empty or not.

It was important to determine the number of molecules in a single transverse slice of the column, one molecule thick. This can be calculated from experimental density and the volume of the slice. The area of the slice is easily obtained from powder X-

dx.doi.org/10.1021/ja3060904 | J. Am. Chem. Soc. 2012, 134, 13871–13880

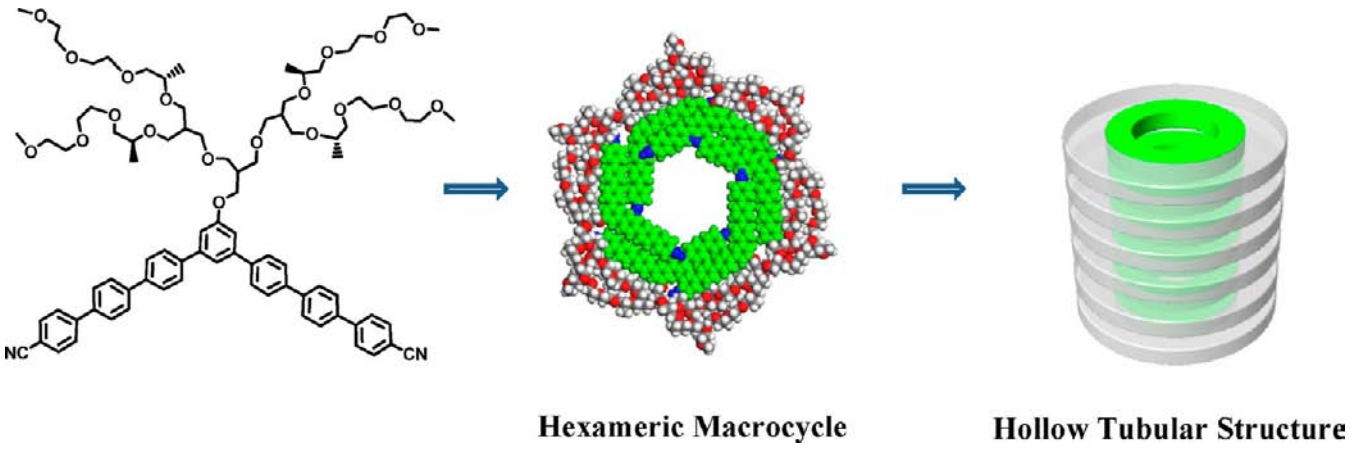

Figure 6. Schematic representation of proposed self-assembly for formation of hexameric macrocycle.

ray diffraction, but the thickness was not clear until oriented fibers of **2** and **3** were prepared by extrusion in a homemade microextruder. As seen in Figures 5c and S2, Supporting Information, the fiber patterns contain sharp equatorial reflections in the small-angle region, matching exactly the hexagonal *hk*0 diffraction peaks in the powder patterns; these correspond to lattice parameters a = 6.34 and 7.43 nm for **2** and **3**, respectively (Tables S2 and S3, Supporting Information). In the wide-angle region, there is a series of closely spaced moderately sharp arcs straddling the meridian. While the degree of orientation of the fiber was insufficient to index these reflections directly based on their ξ,ζ cylindrical reciprocal space coordinates, we could retrieve the *hkl* indices by finding the best-fit c lattice parameter through matching of their measured d spacings (Figure 5d) to those of the first layer line (*hk*1) reflections of a 3D hexagonal unit cell of known a, see Table S6, Supporting Information. The positions of the azimuthally narrowed Bragg arcs corresponding to the matched reflections are depicted in Figure 5e. From this indexing, the c parameter is found to be 0.432 ± 0.004 nm for compounds **2** and **3**. On the basis of the measured density (1.18 and 1.20 g/cm^3 for **2** and **3**–**4**, respectively), we arrive at the average number of molecules in a single slice of the column as 7.1, 8.4, and 9.6 for **2**, **3**, and **4**, respectively (Table S7, Supporting Information). These numbers invalidate the model of hexameric macrocycles and suggest a more disordered arrangement of the aromatic cores.

Reconstruction of Electron Density Maps, and Simulation of Diffraction Patterns. To resolve the question of what is in the center of the columns, a 3-level geometric model of electron density (ED) was built on a 2D hexagonal lattice. The model consisted of a ring of reference electron density ED = 1, the outside continuum with reference ED = 0, and an inner circle, the density of which was an adjustable parameter H (height) or D (depth), respectively, for models I and II. The cross-section ED profiles are shown in Figure 7,b. Both models correspond to a core–shell structure. Fourier coefficients, i.e., diffraction amplitudes, were calculated analytically. The variables (fitting parameters) were the outer and inner radii of the ring and the value of H (D). The two models gave fittings to the experimentally measured intensities with a similar fitting quality R^2 (Table 1 and Tables S8–S10, Supporting Information). However, while the D values from model I varied drastically between the three samples, from −3.29 to −0.77, the H values from model II were rather similar

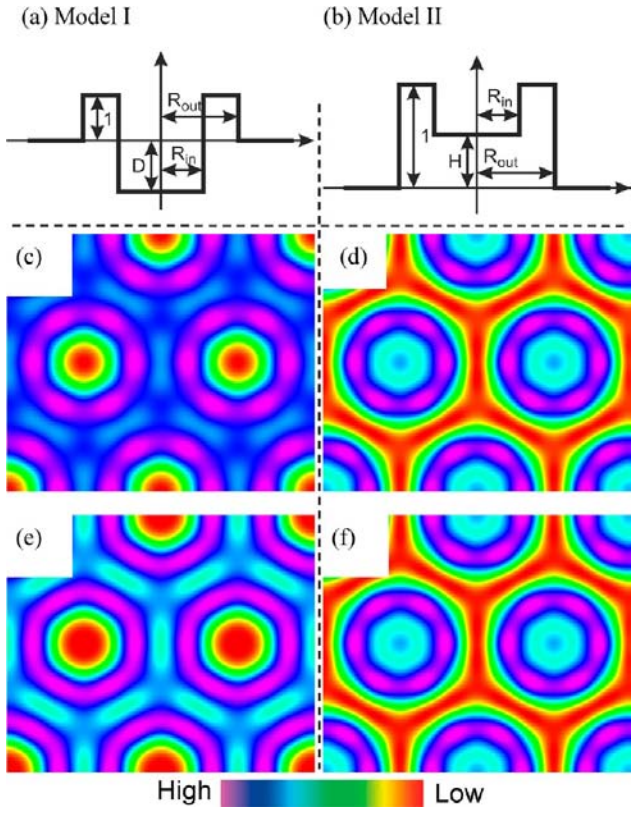

Figure 7. Electron density maps of the hexagonal phase of compound **2**. (a,b) Three-level geometric model of electron density. (c,d) Fourier approximations of models I (a) and II (b) using 5 Fourier terms, the same number as the number of X-ray reflections used in reconstruction of the corresponding experimental maps (e,f). (e,f) Reconstructed from experimental diffraction intensities using phases from best-fit models I (c) and II (d). Match between the model and experiment should be judged by the similarity of the top and bottom maps. Color scale is at the bottom.

for all three samples, ranging only from 0.53 to 0.64 (Table 1). On this basis, it is concluded that model II is the correct representation of the ED profile across the column. Thus, simulation of *hk*0 diffraction intensities supports the model where the periphery of the column is formed by the aromatic backbones (high ED), surrounded both outside and inside by the ethylene-oxide dendrons (lower ED). It should be

dx.doi.org/10.1021/ja3060904 | J. Am. Chem. Soc. 2012, 134, 13871–13880

Table 1. Best-Fit Parameters to Electron Density Models I and II of the Hexagonal Phase of Compounds 2−4 Described in Figure 7[a]

compd	a, nm	model	R_{out}, nm	R_{in}, nm	D or H	R^2 [b]
2	6.34	I	2.34	1.30	−3.29	0.992
		II	2.56	1.25	**0.64**	0.999
3	7.43	I	2.84	1.80	−1.26	0.961
		II	3.02	1.99	**0.62**	0.997
4	8.27	I	3.37	2.15	−0.77	0.988
		II	3.37	2.60	**0.53**	0.956

[a]Five strongest reflections were used. More detailed data and fits to more reflections are listed in Tables S8−S10, Supporting Information. [b]Variance.

mentioned, incidentally, that gravimetric density measurements also favor model II over model I (see previous section).

Fourier approximations of model I and II ED maps using the 5 Fourier terms corresponding to the 5 diffraction peaks used in the model fitting are shown in Figure 7c,d. One way to judge the goodness of the fit of the model is to compare the "smeared" models in Figure 7c,d with the ED maps reconstructed directly from experimental intensities using the same combination of structure factor phases (+ or − signs, Tables S8−S10, Supporting Information). The latter "experimental" maps are shown in Figure 7e,f. For the case of compound **2**, the fit of model II (Figure 7d,f) is somewhat better than that for model I (Figure 7c,d), as also indicated by the R^2 values in Table 1. However, the strongest evidence in favor of model II is the consistency of the ED maps for the three compounds when using the phase combination from model II, see Figure 8. The above analysis illustrates the importance of comparing ED maps and models for a homologous series, rather than for one compound alone.[4c]

Molecular Model. To gain further insight into the columnar structure of **2**−**4**, we again performed MD simulation by placing the calculated number of molecules in a single slice of the columns with the experimentally determined unit cell dimensions. Thus, e.g., to simulate compound **2** seven molecules were arranged in a 60° rhombic prism box with a side length of 6.34 nm and a height of 0.43 nm, under the 3d periodic boundary condition (Figure 9a). This simulation confirms the viability of the structure with seven bent molecules in a single slice packed into a shell of aromatic moieties, with six molecules having their dendritic groups facing outward and one molecule turned around for its dendron to fill the internal pore. In the case of compound **3**, the 8-molecule aggregate with two dendrons facing inward gives good space-filling after MD annealing (Figure 9b), as does the 10-molecule model of compound **4** with four molecules turned inward (not shown). Notably, the number of molecules with the dendrons facing outward remains constant at six for all three compounds. According to the best-fit electron density models, the diameters of the rings of aromatic cores in compounds **2** and **3** are R_{in} + R_{out} = 3.8 and 5.0 nm, respectively. These diameters are in good agreement with the size of the aromatic circles in the MD annealed models in Figure 9a,b. The MD simulations, together with the circular nature of the aromatic shell of the averaged columns, suggest a relatively disordered arrangement of the bent cores around the cylinder. This allows incorporation of numbers of molecules larger than 6 into a column slice, with the extra molecules inverted. This mode of self-assembly avoids the high energy penalty of the hollow tubular structure.

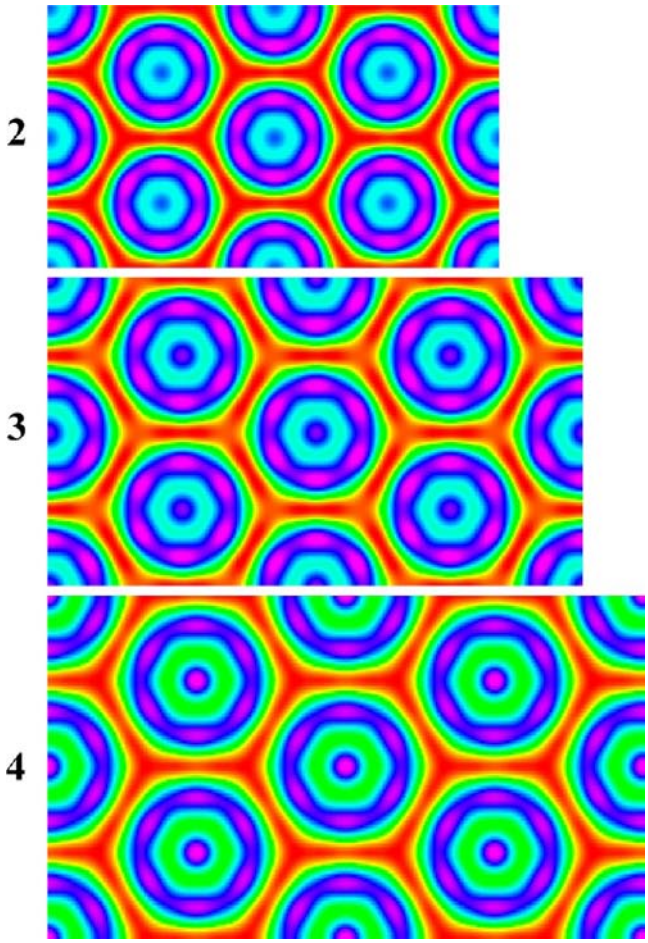

Figure 8. Electron density maps of compounds **2**, **3**, and **4** reconstructed using the first five *hk*0 diffraction peaks with the phase combination +−−++ (+ = 0 rad, − = π rad). This phase combination corresponds to that in model II. Maps are scaled in size proportional to the size of the unit cell.

It is worth remarking at this point that as the fiber patterns of **2** and **3** show (Figures 5c and S2a, Supporting Information), there is in fact weak 3D long-range order in these thermotropic column-like structures, so that one might be tempted to classify them as soft crystals. The distinct *hkl* Bragg reflections indicate weak long-range longitudinal correlation between one-molecule-thick *slices* across different columns. However, in view of the nonuniform structure *within* the column slices, with individual *molecules* not having a uniquely defined preferred position, we still prefer to describe these structures as liquid crystals. It should also be mentioned that a very weak 0.6−0.7 nm reflection is consistently observed close to the meridian, so that the reflections around 0.4 nm may strictly speaking be on the second layer line. The weak 0.6−0.7 nm reflection is in fact commonly observed in "ordered" columnar systems.[5b] In more highly oriented fibers these are seen to be off-meridian and coming from a doubling of the fiber repeat. In the present systems the weak 0.6−0.7 nm feature seems to arise from the herringbone arrangement of phenylene planes with alternating positive and negative tilt along the column.

Lamellar Phase of Compound 3. Notably, compound **3** showed small-angle Bragg diffraction even above the melting temperature at 160 °C. The melting has a comparatively large enthalpy change, and the high-temperature phase appeared fluid in POM, indicating isotropic phase. As seen in Figure 5a,

dx.doi.org/10.1021/ja3060904 | J. Am. Chem. Soc. 2012, 134, 13871−13880

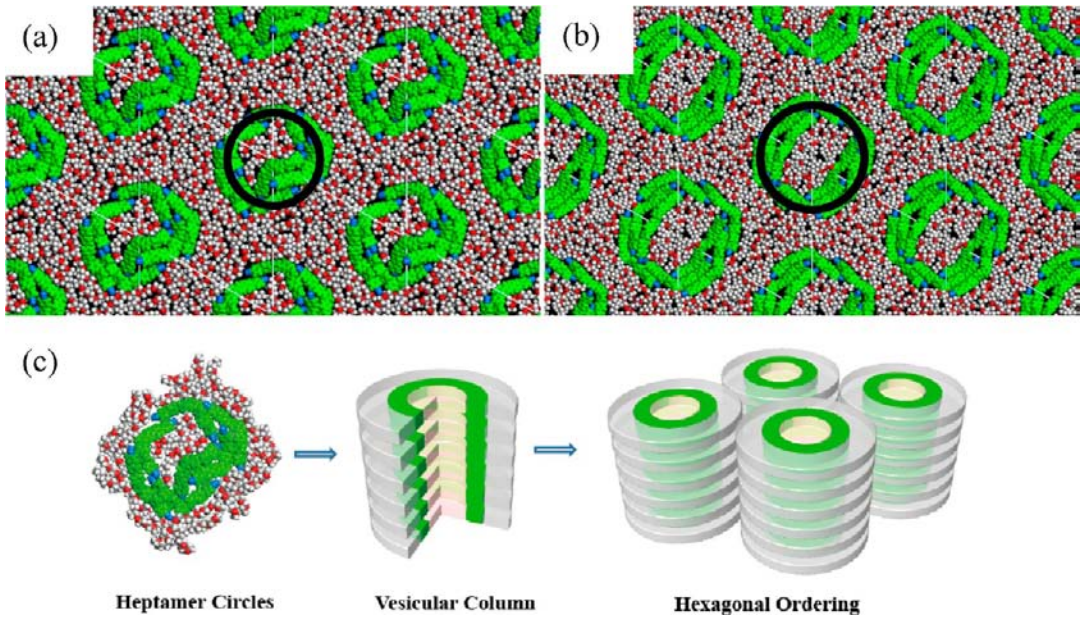

Figure 9. Snapshots of the structures of (a) **2** and (b) **3** after MD annealing (CN ends are colored blue and the bent aromatic cores green). Added black circles have the median diameter (R_{in} + R_{out}) of the high electron density (aromatic) rings in the best-fit model of type II (see Table 1). (c) Schematic representation of formation of the supramolecular channels.

bottom, the two Bragg reflections are the two orders of a 2.42 nm diffraction. The phase is therefore designated as layered, with alternating sublayers of rod segments and aliphatic dendrons. The relatively strong second-order reflection suggests a somewhat unconventional structure, and indeed, the 1D electron density profile has a narrow high-density maximum, purple in Figure 10. This suggest that the aromatic

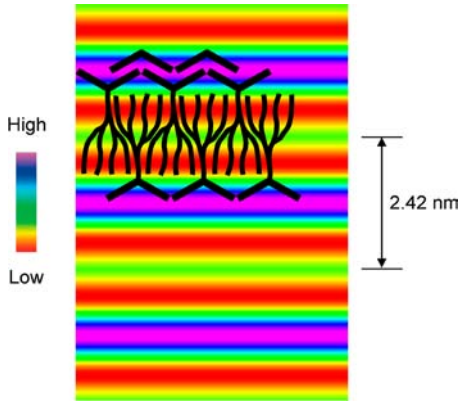

Figure 10. Electron density map of the lamellar phase of compound **3**. Schematic representations of molecules are superimposed. Note that there is no experimental evidence of in-plane periodicity.

rods are oriented parallel to the layer plane (see schematic molecules in Figure 10), similar to the organization in the lamellar phases of thermotropic T-shaped amphiphilic liquid crystals.[4a,14] In fact, the latter have also been observed above the temperature range of honeycomb structures.[4a]

The obvious question posed by the present work is why do compounds **2**–**4** exhibit the vesicular cylinder structure instead of the lamellar structure observed in **3** at high temperatures. Thermotropic mesophases with cylinders or spheres in which most molecules' wide ends face out but some face in have been reported recently in low-taper mesogens and dendrons.[5e] These vesicles can be regarded as highly curved double layers. The usual situation in diblock amphiphiles is a choice between a flat double layer and a column in which all A blocks face inward and all B blocks face outward. Bicontinuous cubic phases, ribbon phases, and undulated bilayers have been observed as alternative solutions to the frustration created by steric imbalance between the two blocks. The new vesicular phases clearly present an alternative solution, and their understanding requires further study.

■ CONCLUSION

We demonstrated that bent molecules externally grafted with a dendritic oligoether chain self-assemble into unique supramolecular channel structures in the bulk. The results described here demonstrate that bent rod molecules **2**–**4** self-assemble into supramolecular channels with both the interior and the exterior filled with the amorphous dendritic side groups. The channels, consisting of between 7 and 10 molecules in cross-section, are arranged on a hexagonal lattice with high in-plane order and weak long-range 3D correlations. Formation of such a channel structure is attributed to the combination of noncovalent interactions within the supramolecular macrocycles and other factors including electrostatic interactions and space filling. Although compound **1** has the same molecular structure as **2** except for the absence of nitrile groups, **1** forms thin columns based on dimers, i.e., with only two molecules in cross-section. Such core–shell columnar structures are well known in rod–coil systems. However, since the bent aromatic core of molecules **2**–**4** were functionalized with terminal nitrile groups, they self-assemble into macrocycles driven by complementary electrostatic interactions between electron-withdrawing nitrile groups and electron-donating phenoxy groups. The resulting cycles are stabilized by additional π–π interactions. Importantly, the aromatic cylinders have large interior spaces, between 2.5 and 5.2 nm in diameter, depending on the length of the bent segments. Although the flexible dendrons are attached to the outer apex of the bent rod, the

inside of the cylinders is filled by such dendrons since some molecules are turned with their convex apex facing inside. Although a few channel-like structures have been reported previously,[4,5] self-assembly of channel-like structures with controllable diameter is rare in material science and macromolecular engineering. We believe that this unique strategy for constructing channels with defined shape and size will result in novel ion transport channels and electro-optic nanomaterials.

■ ASSOCIATED CONTENT

Supporting Information

Synthetic and other experimental details. This material is available free of charge via the Internet at http://pubs.acs.org.

■ AUTHOR INFORMATION

Corresponding Author

g.ungar@sheffield.ac.uk; myongslee@snu.ac.kr

Author Contributions

‡These authors contributed equally.

Notes

The authors declare no competing financial interest.

■ ACKNOWLEDGMENTS

This work was supported by the National Research Foundation of Korea (NRF) grant funded by the Korean government (MEST) (nos. 2012-0001240 and 2011-35B-C00024) and by the European Union FP7 project Nanogold (grant no. 228455). We acknowledge the Pohang Accelerator Laboratory, Korea, and Diamond Light Source, U.K., for allowing us to use the synchrotron source. We acknowledge a fellowship of the BK21 program from the Ministry of Education and Human Resources Development of Korea. G.U. acknowledges support from the WCU program through the National Research Foundation of Korea (R31-10013). For help with the synchrotron experiments we thank Drs. Nick Terrill and Jen Hiller (beamline I22) at Diamond Light Source. We also thank Dr. P. Baker and Prof. D. Rice at the Biochemistry Department, Sheffield, for allowing use of their wide-angle diffraction setup.

■ REFERENCES

(1) (a) Shimizu, T.; Masuda, M.; Minamikawa, H. *Chem. Rev.* **2005**, *105*, 1401−1443. (b) Hill, D. J.; Mio, M. J.; Prince, R. B.; Hughes, T. S.; Moore, J. S. *Chem. Rev.* **2001**, *101*, 3893−4012. (c) Hoeben, F. J. M.; Jonkheijm, P.; Meijer, E. W.; Schenning, A. P. H. J. *Chem. Rev.* **2005**, *105*, 1491−1546. (d) Yamamoto, Y.; Fukushima, T.; Suna, Y.; Ishii, N.; Saeki, A.; Seki, S.; Tagawa, S.; Taniguchi, M.; Kawai, T.; Aida, T. *Science* **2006**, *314*, 1761. (e) Yashima, E.; Maeda, K.; Furusho, Y. *Acc. Chem. Res.* **2008**, *41*, 1166−1180. (f) Praveen, V. K.; George, S. J.; Varghese, R.; Vijayakumar, C.; Ajayaghosh, A. *J. Am. Chem. Soc.* **2006**, *128*, 7542−7550.

(2) (a) Kato, T.; Mizoshita, N.; Kishimoto, K. *Angew. Chem., Int. Ed.* **2006**, *45*, 38−36. (b) Cui, H.; Pashuck, E. T.; Velichko, Y. S.; Weigand, S. J.; Cheetham, A. G.; Newcomb, C. J.; Stupp, S. I. *Science* **2010**, *327*, 555−559. (c) Hartgerink, J. D.; Beniash, E.; Stupp, S. I. *Science* **2001**, *294*, 1684−1688. (d) Miyajima, D.; Tashiro, K.; Araoka, F.; Takezoe, H.; Kim, J.; Kato, K.; Takata, M.; Aida, T. *J. Am. Chem. Soc.* **2009**, *131*, 44−45. (e) van Gorp, J. J.; Vekemans, J. A. J. M.; Meijer, E. W. *J. Am. Chem. Soc.* **2002**, *124*, 14759−14769. (f) Tschierske, C. *Chem. Soc. Rev.* **2007**, *36*, 1930−1970. (g) Soininen, A. J.; Kasëmi, E.; Schlüter, D.; Ikkala, O.; Ruokolainen, J.; Mezzenga, R. *J. Am. Chem. Soc.* **2010**, *132*, 10882−10890. (h) Chung, Y.-W.; Lee, J.-K.; Zin, W.-C.; Cho, B.-K. *J. Am. Chem. Soc.* **2008**, *130*, 7139−7147. (i) Sato, K.; Itoh, Y.; Aida, T. *J. Am. Chem. Soc.* **2011**, *133*, 13767−13769. (j) Ungar, G.; Tschierske, C.; Abetz, V.; Holyst, R.; Bates, M. A.; Liu, F.; Prehm, M.; Kieffer, R.; Zeng, X. B.; Walker, M.; Glettner, B.; Zywocinski, A. *Adv. Funct. Mater.* **2011**, *21*, 1296−1323.

(3) (a) Tahara, K.; Okuhata, S.; Adisoejoso, J.; Lei, S.; Fujita, T.; De Feyter, S.; Tobe, Y. *J. Am. Chem. Soc.* **2009**, *131*, 17583−17590. (b) Ahn, S.; Matzger, A. J. *J. Am. Chem. Soc.* **2010**, *132*, 11364−11371. (c) Kaucher, M. S.; Peterca, M.; Dulcey, A. E.; Kim, A. J.; Vinogradov, S. A.; Hammer, D. A.; Heiney, P. A.; Percec, V. *J. Am. Chem. Soc.* **2007**, *129*, 11698−11699. (d) Sakai, N.; Kamikawa, Y.; Nishii, M.; Matsuoka, T.; Kato, T.; Matile, S. *J. Am. Chem. Soc.* **2006**, *128*, 2218−2219. (e) Ghadiri, M. R.; Granja, J. R.; Milligan, R. A.; McRee, D. E.; Khazanovich, N. *Nature* **1993**, *366*, 324−327. (f) Bong, D. T.; Clark, T. D.; Granja, J. R.; Ghadiri, M. R. *Angew. Chem., Int. Ed.* **2001**, *40*, 988−1011. (g) Reches, M.; Gazit, E. *Science* **2003**, *300*, 625−627. (h) Gazit, E. *Chem. Soc. Rev.* **2007**, *36*, 1263−1269. (i) Fritzsche, M.; Bohle, A.; Dudenko, D.; Baumeister, U.; Sebastiani, D.; Richardt, G.; Spiess, H. W.; Hansen, M. R.; Höger, S. *Angew. Chem., Int. Ed.* **2011**, *50*, 3030−3033.

(4) (a) Prehm, M.; Liu, F.; Baumeister, U.; Zeng, X.; Ungar, G.; Tschierske, C. *Angew. Chem., Int. Ed.* **2007**, *46*, 7972−7975. (b) Cheng, X.; Dong, X.; Wei, G.; Prehm, M.; Tschierske, C. *Angew. Chem., Int. Ed.* **2009**, *48*, 8014−8017. (c) Zeng, X. B.; Kieffer, R.; Glettner, B.; Nürnberger, C.; Liu, F.; Pelz, K.; Prehm, M.; Baumeister, U.; Hahn, H; Lang, H; Gehring, G. A.; Weber, C. H. M.; Hobbs, J. K.; Tschierske, C.; Ungar, G. *Science* **2011**, *331*, 1302−1306.

(5) (a) Percec, V.; Dulcey, A. E.; Balagurusamy, V. S. K.; Miura, Y.; Smidrkal, J.; Peterca, M.; Nummelin, S.; Edlund, U.; Hudson, S. D.; Heiney, P. A.; Hu, D. A.; Magonov, S. N.; Vinogradov, S. A. *Nature* **2004**, *430*, 764−768. (b) Shcherbina, M. A.; Zeng, X. B.; Tadjiev, T.; Ungar, G.; Eichhorn, S. H.; Phillips, K. E. S.; Katz, T. J. *Angew. Chem., Int. Ed.* **2009**, *48*, 7837−7840. (c) Percec, V.; Dulcey, A. E.; Peterca, M.; Ilies, M.; Sienkowska, M. J.; Heiney, P. A. *J. Am. Chem. Soc.* **2005**, *127*, 17902−17909. (d) Percec, V.; Peterca, M.; Dulcey, A. E.; Imam, M. R.; Hudson, S. D.; Nummelin, S.; Adelman, P.; Heiney, P. A. *J. Am. Chem. Soc.* **2008**, *130*, 13079−13094. (e) Peterca, M.; Imam, M. R.; Leowanawat, P.; Rosen, B. M.; Wilson, D. A.; Wilson, C. J.; Zeng, X.; Ungar, G.; Heiney, P. A.; Percec, V. *J. Am. Chem. Soc.* **2010**, *132*, 11288−11305. (f) Percec, V.; et al. *Science* **2010**, *328*, 1009−1014. (g) Peterca, M.; Percec, V.; Leowanawat, P.; Bertin, A. *J. Am. Chem. Soc.* **2011**, *133*, 20507−20520.

(6) (a) Lee, M.; Cho, B.-K.; Zin, W.-C. *Chem. Rev.* **2001**, *101*, 3869−3892. (b) Yang, W.-Y.; Ahn, J.-H.; Yoo, Y.-S.; Oh, N.-K.; Lee, M. *Nat. Mater.* **2005**, *4*, 399−403. (c) Kim, J.-K.; Hong, M.-K.; Ahn, J.-H.; Lee, M. *Angew. Chem., Int. Ed.* **2005**, *44*, 328−332. (d) Ryu, J.-H.; Oh, N.-K.; Zin, W.-C.; Lee, M. *J. Am. Chem. Soc.* **2004**, *126*, 3551−3558. (e) Lee, E.; Huang, Z.-G.; Ryu, J.-H.; Lee, M. *Chem.—Eur. J.* **2008**, *14*, 6957−6966.

(7) (a) Hong, D.-J.; Lee, E.; Jeong, H.; Lee, J.-K.; Zin, W.-C.; Nguyen, T. D.; Glotzer, S. C.; Lee, M. *Angew. Chem., Int. Ed.* **2009**, *48*, 1664−1668. (b) Hong, D.-J.; Lee, E.; Lee, J.-K.; Zin, W.-C.; Han, M.; Sim, E.; Lee, M. *J. Am. Chem. Soc.* **2008**, *130*, 14448−14449. (c) Lee, M.; Park, M.-H.; Oh, N.-K.; Zin, W.-C.; Jung, H.-T.; Yoon, D.-K. *Angew. Chem., Int. Ed.* **2004**, *43*, 6465−6468.

(8) (a) Dantlgraber, G.; Eremin, A.; Diele, S.; Hauser, A.; Kresse, H.; Pelzl, G.; Tschierske, C. *Angew. Chem., Int. Ed.* **2002**, *41*, 2408−2412. (b) Keith, C.; Reddy, R. A.; Hauser, A.; Baumeister, U.; Tschierske, C. *J. Am. Chem. Soc.* **2006**, *128*, 3051−3066.

(9) (a) Kim, H.-J.; Kim, J.-K.; Lee, M. *Chem. Commun.* **2010**, *46*, 1458−1460. (b) Kim, H.-J.; Lee, E.; Park, H.-s.; Lee, M. *J. Am. Chem. Soc.* **2007**, *129*, 10994−10995. (c) Kim, H.-J.; Lee, J.-H.; Lee, M. *Angew. Chem., Int. Ed.* **2005**, *44*, 5810−5814. (d) Kim, H.-J.; Zin, W.-C.; Lee, M. *J. Am. Chem. Soc.* **2004**, *126*, 7009−7014.

(10) (a) Ito, H.; Ikeda, M.; Hasegawa, T.; Furusho., Y.; Yashima, E. *J. Am. Chem. Soc.* **2011**, *133*, 3419−3432. (b) Ikeda, M.; Tanaka, Y.; Hasegawa, T.; Furusho, Y.; Yashima, E. *J. Am. Chem. Soc.* **2006**, *128*, 6806−6807.

(11) Kim, H.-J.; Jeong, Y.-H.; Lee, E.; Lee, M. *J. Am. Chem. Soc.* **2009**, *131*, 17371−17375.

(12) Kim, H.-J.; Kang, S.-K.; Lee, Y.-K.; Seok, C.; Lee, J.-K.; Zin, W.-C.; Lee, M. *Angew. Chem., Int. Ed.* **2010**, *49*, 8471−8475.

(13) (a) Turner, D. C.; Gruner, S. M. *Biochemistry* **1992**, *31*, 1340−1355. (b) Rappolt, M.; Hickel, A.; Bringezu, F.; Lohner, K. *Biophys. J.* **2003**, *84*, 3111−3122.
(14) (a) Cheng, X. H.; Prehm, M.; Das, M. K.; Kain, J.; Baumeister, U.; Diele, S.; Leine, D.; Blume, A.; Tschierske, C. *J. Am. Chem. Soc.* **2003**, *125*, 10977−10996. (b) Patel, N. M.; Syed, I. M.; Rosenblatt, C.; Prehm, M.; Tschierske, C. *Liq. Cryst.* **2005**, *32*, 55−61.